# Anharmonic bend-stretch coupling in neat liquid water

Lindner, Joerg; Cringus, Dan; Pshenichnikov, Maxim S.; Voehringer, Peter

*Published in:*
Chemical Physics

*DOI:*
10.1016/j.chemphys.2007.07.051



*Publication date:*
2007

Available online at www.sciencedirect.com
ScienceDirect
Chemical Physics 341 (2007) 326–335
Chemical Physics
www.elsevier.com/locate/chemphys

# Anharmonic bend–stretch coupling in neat liquid water

Jörg Lindner [a,*], Dan Cringus [b], Maxim S. Pshenichnikov [b], Peter Vöhringer [a]

[a] Lehrstuhl für Molekulare Physikalische Chemie, Institut für Physikalische und Theoretische Chemie, Rheinische Friedrich-Wilhelms-Universität, Wegelerstraße 12, 53115 Bonn, Germany
[b] Department of Physical Chemistry, Zernike Institute for Advanced Materials, University of Groningen, Nijenborgh 4, 9747 AG Groningen, The Netherlands

Received 10 May 2007; accepted 31 July 2007
Available online 10 August 2007

**Abstract**

Femtosecond mid-IR spectroscopy is used to study the vibrational relaxation dynamics in neat liquid water. By exciting the bending vibration and probing the stretching mode, it is possible to reliably determine the bending and librational lifetimes of water. The anharmonic coupling between the bending and the stretching degrees of freedom is quantified in terms of a differential absorption cross-section for the fundamental stretching transition carrying one spectating bending quantum. A positive off-diagonal anharmonicity may be caused by the initial excitation of the anharmonic bending mode and is mediated by the hydrogen bonded network.


*Keywords:* Liquid; Water; Ultrashort time-resolved mid-infrared spectroscopy; Vibrational relaxation

## 1. Introduction

Nonlinear infrared (IR) spectroscopy is currently one of the most powerful methods capable to obtain detailed insight into the dynamics of hydrogen-bonded molecular liquids in real time [1,2]. In neat liquid water, the relaxation dynamics associated with vibrational excitations are governed by a complex interplay between intramolecular degrees of freedom (bending and two stretching modes) on one hand and intermolecular modes of the liquid with both single-molecule and collective character on the other. Both classes of vibrational motions contribute to structural fluctuations of an extended three-dimensional random hydrogen-bond network [3], covering time-scales from several picoseconds down to a few tens of femtoseconds. Interestingly, their mutual couplings cause the frequencies of the fundamental intramolecular modes to be considerably shifted and the corresponding resonances to be extremely broadened as compared to the gas-phase, making them attractive and highly sensitive spectroscopic probes for dynamical disorder and energy flow processes in the hydrogen-bond network. An IF absorption spectrum of pure liquid water is shown in Fig. 1.

First femtosecond infrared experiments with sufficient time-resolution to study vibrational relaxation in neat liquid water were carried out by Bakker and coworkers [4,5]. The OH-stretching mode was found to relax to an intermediate state with a time-constant of approximately 200 fs. The intermediate state was speculated to be the first excited state of the bending vibration.

From IR-experiments on $H_2O$–$D_2O$ mixtures, a lifetime of the $H_2O$ bending vibrations of 400 fs was derived [6]. This value is however questionable, because of substantial background absorptions from the bending vibration of $D_2O$ and HOD in the region of the $H_2O$ bend. Indeed, by exciting and probing the same bending vibration of neat liquid $H_2O$, a considerably shorter lifetime of 170 fs was identified by Elsaesser and coworkers [7]. In parallel, from an IR echo study in the OH-stretching region, spectral diffusion was monitored in neat liquid $H_2O$ on an ultrashort time scale of 50 fs [8].

* Corresponding author. Tel.: +49 228 73 7055; fax: +49 228 73 7049.
*E-mail addresses:* jlindner@uni-bonn.de (J. Lindner), M.S.Pchenitchnikov@RuG.nl (M.S. Pshenichnikov).

0301-0104/$ - see front matter © 2007 Elsevier B.V. All rights reserved.
doi:10.1016/j.chemphys.2007.07.051

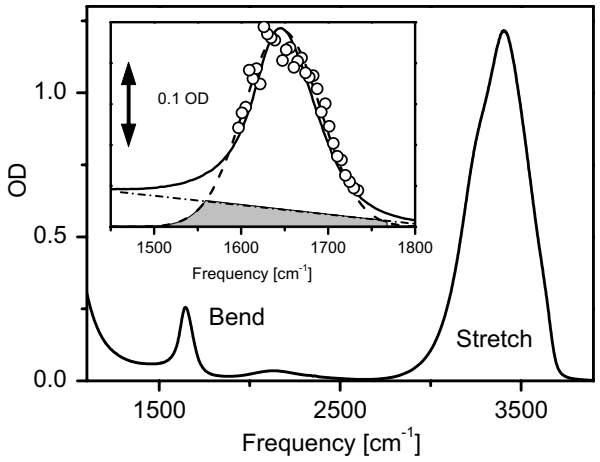


Fig. 1. Absorption spectrum of pure liquid water in the mid-infrared. Inset: Bending mode absorption (solid line) and pump-pulse spectrum (open circles). Noise-like spikes originate from non-uniform amplifications of the electrical signals from the individual pixels of the detector. The dashed line is a fit of a Gaussian spectral profile to the pump-pulse spectrum. The shaded region estimates the background from an underlying continuum.

So far, most time-resolved studies in the mid-IR on vibrational dynamics in liquid $H_2O$ remained limited to "quasi degenerate" experiments, in which the center frequencies of the pump and probe were tuned to the same resonance, i.e. either the bending or the stretching vibration. To reveal the relaxation dynamics and pathways as well as the spectroscopically relevant IR-active transitions in a more comprehensive fashion, we recently focused on a multicolor approach covering both the bending and stretching spectral region simultaneously in a single measurement [9]. We reported fs-mid-IR data also from the other two excitation combinations, namely: (i) pumping the stretch and probing the bend and (ii) pumping the bend and probing the stretch. Together with the two "degenerate" combinations and globally fitting the entire data set from all four possible pump probe schemes at the same time, we extracted a lifetime of the bending mode of 260 fs and for the stretching mode of 240 fs. In addition, we determined an average lifetime for excitations of the librational modes (i.e. the hindered rotational manifold) of 780 fs. Furthermore, such a global analysis naturally provided a comprehensive picture for the network of relaxation pathways connecting the bending and stretching vibrational manifolds [9]. Finally, in a similar sprint, Ashihara et al. reported fs-IR-studies, which probe the librational-to-bending spectral region from 600 to 1700 $cm^{-1}$ following an initial librational, bending, or stretching excitation of neat liquid water [10,11]. Stretching and bending lifetimes of 200 and 170 fs were determined, which are slightly shorter than those reported by Bakker [4,5] and in our communication [9], respectively. Whether or not all data were fitted globally with a common kinetic model was not specified in Ref. [10,11]. Therefore, the slight deviation to our study may be due to the highly stringent convergence criterium for our simulation algorithm simply due to the vast number of experimental data points to be reproduced at the same time.

The key challenge in extracting reliable dynamical parameters from an analysis of the fs-IR-experiments on $H_2O$ lies in the determination of absorption cross-sections and differences thereof of all relevant spectroscopic transitions. In this context, the importance of anharmonic coupling between the bending and the stretching vibrational degrees of freedom has largely escaped attention. It turns out, that the knowledge of the stretch–bend interaction in terms of frequency-dependent absorption cross-sections involving combination tone transitions provides additional and highly valuable clues regarding the nature of the intermediate states that can be transiently populated from an initial OH-stretching quantum [4,5,9].

Early attempts to extract the cross-section for a fundamental stretching excitation carrying one quantum in the bending coordinate due to relaxation from an initially prepared OH-stretching quantum proved to be highly difficult for two reasons [5]: first, the spectral distortion of the OH-stretching resonance by the bending absorption is obscured by the pronounced temporal evolution of the transient differential transmission due to the depopulation kinetics at early times. Second, the pump–probe response is overwhelmed by contributions originating from thermal heating of the liquid at later times [4,5].

We stress, that insufficient knowledge of the anharmonic coupling is a serious issue for an unambiguous interpretation of more sophisticated fs-IR-methods, like two-dimensional IR or IR echo spectroscopies [8]. For example, because of rapid deactivation of an initial OH-stretching excitation into one or two bending quanta, an echo experiment on $H_2O$ not only probes the fluctuations of the fundamental OH stretching transition frequency but also those of its combination tone with the bending mode, i.e. the transition from one initially populated bending quantum to one bending and one stretching quantum excited in the same molecule.

Here, we report on an alternative approach to reveal the bend–stretch anharmonic coupling and present a more detailed account of our procedure to obtain the frequency dependent absorption cross-section related to a stretching excitation accompanied by one spectating bending quantum. The bending mode of liquid $H_2O$ is directly excited by a resonant IR pump pulse and the pump-induced spectro-temporal evolution is monitored in the OH-stretching region. Hence, the experiments reported herein are complementary to those pumping the OH-stretching vibration except that the primary relaxation dynamics from the stretch to the bend are essentially mimicked by the initial "quasi"-instantaneous excitation. Therefore, their dynamic spectral fingerprints are effectively eliminated from the pump–probe response in the OH-stretching region, making our data a critical test for the existing values of the bending and librational lifetimes in liquid water.

## 2. Experimental setup

Pump–probe measurements on neat liquid water were carried out with a tunable dual color mid-infrared femtosecond light source. Laser pulses centered at 780 nm wavelength with an autocorrelation width of 200 fs were obtained from a home-built Ti:sapphire regenerative chirped pulse amplifier system (CPA) seeded with the output of a commercial frequency doubled mode-locked Erbium fiber laser (Imra A-10-SP). The CPA-pulses had energies as high as 800 μJ at a repetition rate of 1 kHz and were used to synchronously pump two optical parametric amplifiers (OPA) (Light Conversion, TOPAS) with a power ratio of 1:2. The power of their combined signal and idler output was 45 and 100 μJ, respectively.

Each OPA output was directed to a home-built difference-frequency generator (DFG) to produce femtosecond mid-IR pulses tunable between 1100 and 3600 $cm^{-1}$. One of the OPA/DFG devices was tuned to the frequency of maximum absorbance of the bending mode of water, thereby providing pump pulses at 1650 $cm^{-1}$ with typical energies of 2.5 μJ, whose spectral width of ~110 $cm^{-1}$ (FWHM) is well matched to the bandwidth of the absorption of the bending mode (see Fig. 1, inset). The other OPA/DFG pair served as probe source with pulse energies of ~2 μJ. The cross-correlation width of the pulses from the two OPA/DFG devices was determined to 260 fs. The probe pulses were attenuated with a combination of half-wave plate and wire-grid polarizer to less than 10% of the pump-pulse energy. The relative polarization between pump and probe pulses was set to magic angle to eliminate signal contributions originating from rotational reorientation dynamics. A reference beam was derived from the probe beam with a 50% beam splitter. The pump, probe, and reference beams were focused and spatially overlapped in the sample with an Au-coated off-axis parabolic mirror (Janos, 10 cm effective focal length). Another identical Au-parabola served to collimate the beams behind the sample and to direct the probe and reference pulses via 10 cm focal length $CaF_2$ lenses to a monochromator (0.2 m, AMKO), whose exit plane was equipped with a 32 pixel dual-row MCT detector array (Infrared Associates). The spectral resolution per pixel is 16 nm and the absolute wavelength accuracy is about one pixel. Because of the bandwidth limitation of our detection pulses to about 150 $cm^{-1}$ (FWHM), the OPA/DFG unit had to be tuned in three increments from ~3100 to 3600 $cm^{-1}$ to cover the entire OH-stretching spectral region of $H_2O$.

The liquid water sample was contained at room temperature in a rotating cell with $CaF_2$ windows separated by a 2 μm thick Teflon-spacer. The sample had maximum optical densities of ~1.2 and ~0.2 in the stretching and bending spectral regions, respectively. Non-resonant signal contributions around zero time-delay originating from the cell windows were recorded independently in an empty cell and subtracted from the raw $H_2O$ data. The complete data set consists of 40 time-resolved pump–probe signals, equivalent to a total of 200 transient differential transmission spectra, covering a temporal window of 10 ps and a spectral window from ~3000 to 3700 $cm^{-1}$.

## 3. Results and discussion

### 3.1. Experimental data

Representative pump–probe temporal traces are shown in Fig. 2 and transient differential transmission spectra for various pump–probe delays are displayed in Fig. 3. In the time domain, nearly all signals asymptotically approach a constant value for ΔOD on a common time scale of roughly 3 ps. This quantitative overall agreement on long time scales implies that the same relaxation dynamics determine the behavior of ΔOD, regardless of the sign of the pump-induced optical density (i.e. transient bleach or induced absorption). An important feature that characterizes all the transients is that an induced signal in the stretching region appears upon bend excitation within our time-resolution. An appearance of such a prompt signal requires the bending and stretching modes to be anharmonically coupled such that induced absorptions are not canceled by transient bleaches, as is the case for a system consisting of two unlike and uncoupled harmonic oscillators.

Those transients in Fig. 2 that are governed by an overall bleach (i.e. negative ΔOD) approach the long time limiting value of ΔOD in a practically single-exponential fashion with a time constant of ~0.8 ps. In contrast, temporal traces exhibiting a net transient absorption (i.e. positive ΔOD) reach the asymptotic ΔOD in a pronounced non-exponential manner. Previous publications [4,5,7,9,10] have unambiguously shown, that the dynamics on a picosecond time-scale reflect the thermalization of the initially deposited pump energy such that the pump–probe focal volume is canonically heated. Thermal stationary difference spectra of water (i.e. temperature induced spectral changes

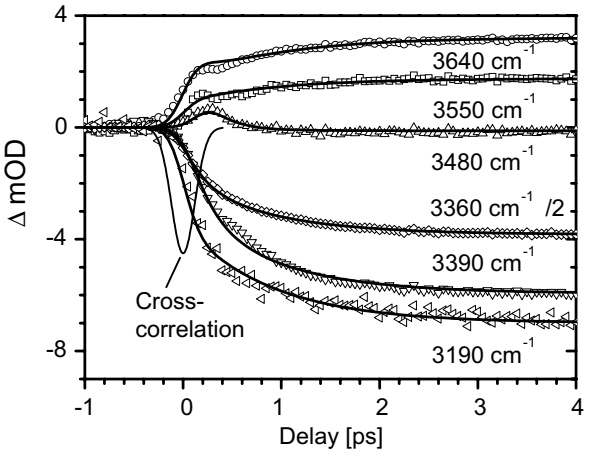


Fig. 2. Typical transients at six different probe frequencies and cross-correlation function.

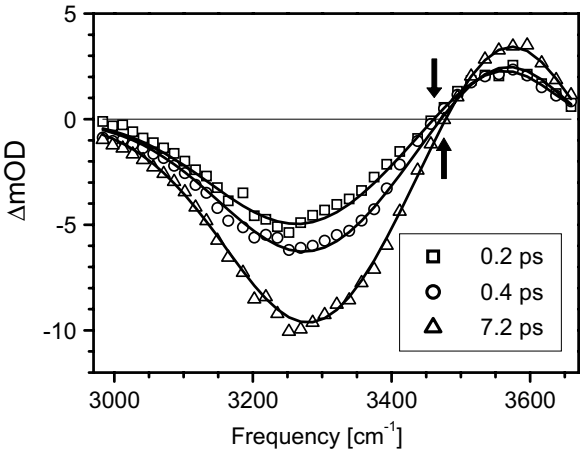


Fig. 3. Transient spectra at various delay times. Frequencies for which $\Delta OD = 0$ are indicated with arrows, for details see text.

in the OH-stretching region) monitored through linear FTIR absorption spectroscopy reveal that this heating effect becomes almost negligible for frequencies around 3480 $cm^{-1}$. A pump–probe transient recorded at exactly this frequency (Fig. 2) is characterized by a pulse-width limited rise of a transient absorption and a subsequent decay, which yields a time constant after deconvolution of 220 fs. In our previous publication [9], we reported a preliminary decay time of 260 fs and assigned it to the lifetime of the first excited state of the bending mode because of the insensitivity of this transient to heating effects.

In the frequency domain (see Fig. 3), the pump-induced optical density in the OH-stretching region is governed by a bleach centered at ~3300 $cm^{-1}$. Such a bleach is expected for non-vanishing off-diagonal bend–stretch anharmonicity because of the ground-state depletion by the pump-pulse, which is on resonance with the bending vibration. More surprisingly, a transient absorption is observed, which is shifted to higher frequencies with respect to the ground-state bleach. Such an observation is even more surprising because it appears blue-shifted even at the earliest pump–probe time-delay before thermalization and sample heating can occur. For infinite delays, this transient absorption around 3600 $cm^{-1}$ spectrally coincides with an absorption feature seen in thermal FTIR difference spectra, clearly evidencing that at such long delays, it originates from sample heating. However, we stress that at the earliest delays (i.e. shorter than the bending mode lifetime of 220 fs) the blue shifted transient absorption spectrum cannot be thermal in nature. Rather, it must be due to effects that are specifically connected to the existence of the bending quantum. Such an interpretation is further substantiated by the time-dependence of the spectral position of vanishing $\Delta OD$, i.e. $\nu_{\Delta OD=0}(\tau)$. As highlighted in Fig. 3 by the vertical arrows, this frequency shifts from 3456 $cm^{-1}$ at a pump–probe delay of 200 fs to 3480 $cm^{-1}$ at 1 ps. The total shift occurs within the spectral width of our probe pulses but it is well in excess of our spectral resolution. Most importantly, when this frequency shift $\nu_{\Delta OD=0}(\tau) - \nu_{\Delta OD=0}(\infty)$ is plotted versus the pump–probe delay, $\tau$, (see Fig. 4) and fitted to an exponential rise according to

$$\nu_{\Delta OD=0}(\tau) - \nu_{\Delta OD=0}(\infty) = [\nu_{\Delta OD=0}(0) - \nu_{\Delta OD=0}(\infty)] \exp\left(\frac{-\tau}{\tau_{FS}}\right) \quad (1)$$

a frequency-shift correlation time of $\tau_{FS} = 220$ fs is obtained, which is indeed identical to the bending mode lifetime. To reiterate, the underlying nature of the transient absorption, which is detected at probe frequencies higher than the ground-state bleach, is clearly changing on the time-scale of the bending mode lifetime. At early times, it is related to the coupling of the bending excitation to the OH-stretching resonance whereas at later times, it is entirely due to sample heating.

Therefore, a kinetic model designed to reproduce the spectro-temporal evolution in the OH-stretching region following an initial preparation of the bending quantum must include the following elementary steps:

First, immediately after bending excitation by the pump-pulse, the transient differential transmission is defined by the product of population in the first excited state of the bending mode and the probe-frequency dependent absorption cross-section for a fundamental stretching transition carrying a single bending quantum, $\sigma_{01-11}$. Here the indices $ij–kl = 01–11$ refer to the quantum numbers of the stretching ($i$ and $k$) and the bending vibrational states ($j$ and $l$), that are coupled by the probe field. In addition, at zero time delay, a bleaching component proportional to the ground state population depletion and the frequency-dependent absorption cross-section for the pure fundamental OH-stretch, $\sigma_{00-10}$, also contributes to

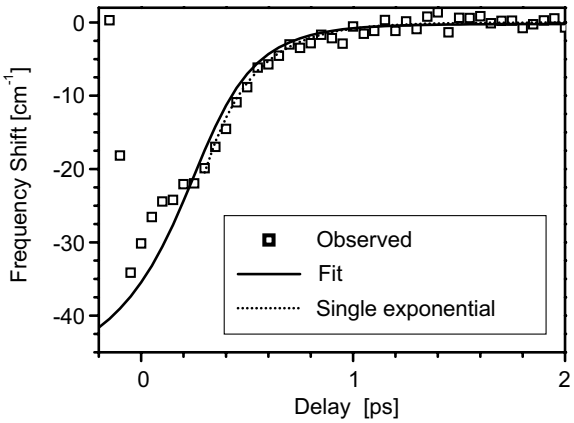


Fig. 4. Time-dependent spectral shift $\nu_{\Delta OD=0}(\tau) - \nu_{\Delta OD=0}(\infty)$ of vanishing differential optical density. Experimental points are shown as open symbols and were obtained by linear regression from six adjacent pixels of the MCT-array for a given time-delay. The solid and the dashed curves depict results from the full numerical simulation and a simple single exponential fit with a time constant of $\tau_{FS} = 220$ fs (Eq. (1)). Note, only the tail was fitted for the single exponential to avoid perturbations from the finite instrument response.

the pump-induced optical density, provided the bending and stretching modes are anharmonically coupled. The difference between the two cross-sections, $\sigma_{01-11}-\sigma_{00-01}$, is termed anharmonic coupling cross-section, $\Delta\sigma_{SB}$, and is related to the off-diagonal anharmonicity between the intramolecular bending and stretching degrees of freedom.

Second, bending relaxation sets in possibly populating intermediate states within the energetically highly dispersed librational manifold. A transient occurrence of a librational excitation might help explain the non-exponential temporal behavior of $\Delta OD(\tau)$ seen in the induced absorption region as well as a significantly slower build-up of the thermalization signal as compared to the bending mode decay.

Third, low frequency modes (LFM) will eventually be populated either directly from the first excited state of the bending mode or via intermediate states such as those described above. Population of the LFM is synonymous with thermal heating of the sample. The cross-section required for simulating this heating effect is denoted $\sigma^*_{00-10}$, its difference, $\Delta\sigma_{hot} = \sigma^*_{00-10} - \sigma_{00-10}$ to a steady state spectrum at room temperature can be taken from thermal difference FTIR spectra recorded independently. Note here that a spectral shift $\nu_{\Delta OD=0}(\tau) - \nu_{\Delta OD=0}(\infty)$ of vanishing $\Delta OD$ as displayed in Fig. 4 follows quite naturally if the frequency dependencies of the anharmonic coupling cross-section $\Delta\sigma_{SB}$ and the thermal difference cross-section $\Delta\sigma_{hot}$ are different.

We mention that our model does not include a pump-induced excitation of librational modes. These modes give rise to absorptions below 1000 $cm^{-1}$ and possibly also to a broad background absorption underlying the bending fundamental as indicated in Fig. 1 (inset). A numerical simulation conservatively estimates an excitation of the librational continuum to less than 10%. In a previous publication, Elsaesser and coworkers have specifically observed an additional kinetic component with a time constant of 430 fs when exciting with pump pulses whose center frequency was red-shifted with respect to the bending mode. Such a time constant was never observed in our experiments indicating that librational excitation is indeed negligible.

### 3.2. Kinetic model and fitting procedure

The experimental observations described in the previous section will be analyzed in terms of the relaxation model sketched in Fig. 5. The pump pulse on resonance with the fundamental bending transition experiences the absorption cross-section $\sigma_{00-01}$ and promotes a fraction of the molecules to the first excited state of the bending mode, $|01\rangle$, B in abbreviated form. For the sake of generality, the vibrational relaxations of a bending quantum, B, and a librational quantum, L, proceed along various pathways summarized by the following set of inelastic many-particle interactions:

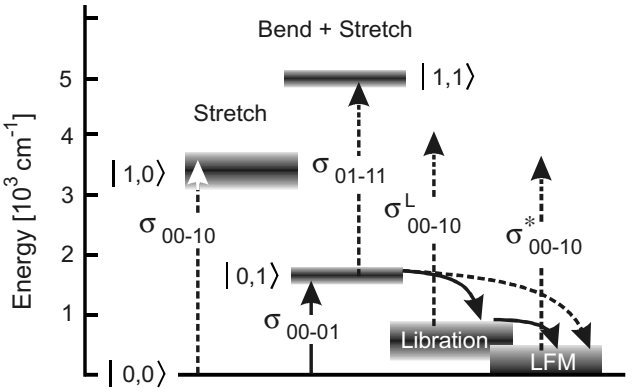


Fig. 5. Energy level diagram of the kinetic model for vibrational relaxation in liquid water following excitation of the bending mode. Abbreviations for cross-sections used in the text: $\Delta\sigma_{SB} = \sigma_{01-11}-\sigma_{00-10}$, $\Delta\sigma_L = \sigma^L_{00-10} - \sigma_{00-10}$, and $\Delta\sigma_{hot} = \sigma^*_{00-10} - \sigma_{00-10}$. The solid line with arrow denotes the excitation of the bending modes, while probed transitions are labeled with dashed lines and an arrow.

$$\begin{aligned}
&\text{(i)}\ \mathrm{B} \xrightarrow{k_1} l_1\mathrm{L} + (l_1-1)\mathrm{H}\\
&\text{(ii)}\ \mathrm{B} \xrightarrow{k_2} l_2\mathrm{L} + m_2\mathrm{M} + (l_2+m_2-1)\mathrm{H}\\
&\text{(iii)}\ \mathrm{B} \xrightarrow{k_3} m_3\mathrm{M} + (m_3-1)\mathrm{H}\\
&\text{(iv)}\ \mathrm{L} \xrightarrow{k_4} m_4\mathrm{M} + (m_4-1)\mathrm{H}
\end{aligned} \tag{2}$$

H denotes a ground state hole and M is an excitation on a low-frequency mode. Path (i) refers to the splitting of the bending excitation into single librational quanta partitioned over $l_1$ water molecules. In the harmonic approximation, the absorption from $l_1$ particles, each of which carrying a single quantum excitation in a given vibration, is indistinguishable from the absorption of a single particle carrying $l_1$ quanta in the same mode. Hence, in this limit, path (i) also represents the generation of high lying excited states of the libration, formerly termed librational overtones [7,10]. Path (ii) on the other hand leads to the transfer of the bending energy onto $l_2$ particles with their libration singly excited or alternatively, onto one water molecule in its $(l_2-1)$th overtone of the libration. The remaining energy (or the energy mismatch with respect to the fundamental bending quantum) is stored into $m_2$ particles carrying a single quantum of excitation in the low frequency modes, M. Alternatively, this energy may be taken up by a single $H_2O$ molecule, whose low frequency mode is then $m_2$-fold excited. Again, in the harmonic limit, the absorption resulting from these two different cases is indistinguishable. In other words, path (ii) leads to a direct production of heat by the decaying bending excited state. This path is however to be differentiated from pathway (iii), which also leads to a direct heating of the liquid by the relaxing bending mode, yet without creating an excitation of the hindered rotations. Finally, pathway (iv) effectively converts librational excitations into single low-frequency mode excitations on $m_4$ particles and can be regarded as a delayed heat production mechanism with the librations serving as the intermediate state.

Using the pathways (i)–(iv) in Eq. (2), the vibrational relaxation dynamics are essentially cast into a sequence of pseudo first-order reactions that fulfill the following set of coupled differential equations:

$$\begin{aligned}\frac{d[B]}{dt} &= -k_B[B],\\ \frac{d[L]}{dt} &= k_{BL}[B] - k_L[L],\\ \frac{d[M]}{dt} &= k_{BM}[B] + m_4 k_L[L],\\ \frac{d[H]}{dt} &= (k_{BL} + k_{BM} - k_B)[B] + (m_4 - 1)k_L[L],\end{aligned} \tag{3}$$

where the rectangular brackets denote time-dependent populations. In particular, the expression $d[H]/dt$ from Eq. (3) represents the creation rate of ground states holes, H, either directly from deactivation of the bending excited state (Eq. (2), paths (i)–(iii)) or through decay of the intermediate libration (Eq. (2), path (iv)). In Eq. (2), $1/k_B$ is the lifetime of the bending mode and $k_B$ is equal to the sum of the pseudo-first-order rate coefficients, $k_i$, for paths $i = 1$, 2, and 3, i.e.

$$k_B = k_1 + k_2 + k_3. \tag{4}$$

Furthermore, $1/k_L$ is the lifetime of the libration given by the pseudo first-order rate constant for path (iv), i.e.

$$k_L = k_4 \tag{5}$$

The quantity $k_{BL}$ represents an effective rate constant for creation of librational excitations from the original bending quantum and is given by the sum over the pseudo-first-order rate coefficients for paths (i) and (ii) (Eq. (2)), each of which weighted by their proper librational stochiometric factors $l_i$:

$$k_{BL} = l_1 k_1 + l_2 k_2. \tag{6}$$

Likewise, the quantity $k_{BM}$ is an effective rate constant for heat production from the initially prepared bending excited state and is calculated as a sum over the pseudo first-order rate coefficients of paths (ii) and (iii) in Eq. (2) however, now weighted by their proper stochiometric factors, $m_i$, for excitation of LFM:

$$k_{BM} = m_2 k_2 + m_3 k_3. \tag{7}$$

The coupled differential equations Eq. (3) can be solved analytically, thereby yielding the time-dependent populations in the form

$$\begin{aligned}[B] &= [B]_0 \exp(-k_B t)\\ [L] &= [B]_0 \frac{k_{BL}}{k_B - k_L}\{\exp(-k_L t) - \exp(-k_B t)\}\\ [M] &= \frac{[B]_0}{k_B}\left\{\left(\frac{m_4 k_L k_{BL}}{k_B - k_L} - k_{BM}\right)\exp(-k_B t) + \left(k_{BM} + m_4 k_{BL}\left[1 - \frac{k_B}{k_B - k_L}\exp(-k_L t)\right]\right)\right\}\end{aligned} \tag{8}$$

and specifically for the ground-state holes

$$\frac{[H]}{[B]_0} = \left\{\frac{(m_4 k_L - k_B)k_{BL}}{k_B(k_B - k_L)} - \frac{k_{BM}}{k_B} + 1\right\}\exp(-k_B t) + \frac{k_{BL}(1 - m_4)}{k_B - k_L}\exp(-k_L t) + \left\{\frac{k_{BM} + m_4 k_{BL}}{k_B} - 1\right\}. \tag{9}$$

The solutions obey particle–hole balance such that

$$[B] + [L] + [M] = [H] + 1 \tag{10}$$

for all times, where the one results from the initial creation of a ground state hole at $t = 0$ by the pump-pulse.

The path-length normalized pump-induced optical density of the sample is then given by

$$\Delta OD = \sigma_{01\text{–}11}[B] + \sigma^{L}_{00\text{–}10}[L] + \sigma^{*}_{00\text{–}10}[M] - \sigma_{00\text{–}01}([H] + 1), \tag{11}$$

where the first term represents the transient absorption of the OH-stretching region of water molecules carrying a single bending quantum. Similarly, the second and third terms result from the OH-stretching absorptions of molecules whose librations and low-frequency modes are excited. Finally, the last term represents the ground-state bleach due to prompt excitation by the pump-pulse and to delayed excitation via energy transfer with vibrationally excited $H_2O$ molecules. Using the particle–hole balance (Eqs. (10) and (11) can be rewritten:

$$\Delta OD = \Delta\sigma_{SB}[B] + \Delta\sigma_{SL}[L] + \Delta\sigma_{hot}[M], \tag{12}$$

where $\Delta\sigma_{SB} = \sigma_{01\text{–}11} - \sigma_{00\text{–}10}$ is the anharmonic stretch–bend cross-section introduced earlier. The quantity $\Delta\sigma_{SL} = \sigma^{L}_{01\text{–}11} - \sigma_{00\text{–}10}$ is the equivalent stretch-libration coupling cross-section and $\Delta\sigma_{hot} = \sigma^{*}_{00\text{–}10} - \sigma_{00\text{–}10}$ is the thermal difference cross-section, which in principle can be obtained from temperature-dependent stationary FT-IR spectra of water.

Apart from these probe-frequency dependent cross-sections, there are nine unknown parameters, which can potentially serve as fitting parameters in simulating the spectro-temporal response in the mid-IR. These are the four rate coefficients $k_i$ contributing to the bending and librational lifetimes, $1/k_B$ and $1/k_L$, the four stoichiometric factors, $l_1$, $l_2$, $m_2$ and $m_3$ determining the effective rate constants, $1/k_{BL}$ and $1/k_{BM}$, and finally the number $m_4$ of low-frequency quanta resulting from the librational decay (path (iv), Eq. (2)). Note that these parameters are frequency-independent and should therefore be used as global quantities that are common to all pump–probe transients regardless of their detection wavelength.

To reduce this large number of free floating fitting parameters in the simulation, it is instructive to simplify the general model outlined in scheme Eq. (2). Assuming that the bending decay is always connected with the simultaneous creation of librational and low-frequency excitations, paths (i) and (iii) can be neglected and the rate coefficients $k_1$ and $k_3$ vanish. In this case, it follows that

$$k_B = \frac{k_{BL}}{l_2} = \frac{k_{BM}}{m_2}. \tag{13}$$

This is identical to assuming that the creation of excitations on the librational and low-frequency modes from the bending excited state is described by the same rate constant. We then introduce the number of low-frequency quanta created directly from the bending quantum, $n_d = m_2$ or indirectly from one bending quantum via librations, $n_i = l_2 m_4$. With the total number of low-frequency quanta, $n_t = n_d + n_i$, one obtains the quantum fractions of directly and indirectly produced excitations according to $P_d = n_d/n_t$ and $P_i = n_i/n_t = 1 - P_d$. We further define the quantum ratio of low-frequency and librational excitations that can be generated from the direct path (ii) as $\Phi = \frac{m_2}{l_2} = \frac{n_d}{l_2}$. This yields the time-dependent populations in the following convenient form:

$$\begin{aligned}
[B] &= [B]_0 \exp(-k_B t),\\
[L] &= [B]_0 \frac{P_d}{\Phi} \frac{k_B}{k_B - k_L}(\exp(-k_L t) - \exp(-k_B t)),\\
[M] &= [B]_0 \left\{ \left( \frac{k_L}{k_B - k_L}(1 - P_d) - P_d \right) \exp(-k_B t) \right.\\
&\quad \left. - \frac{k_B}{k_B - k_L}(1 - P_d)\exp(-k_L t) + 1 \right\},
\end{aligned} \tag{14}$$

and an equivalent expression for [H] results from the particle–hole balance Eq. (10). The convolution with a temporal Gaussian instrument response function can be performed analytically. Under these assumptions, the total number of global fitting parameters is reduced to four, namely $P_d$, $k_L$, $k_B$, and $\Phi$. From the mid-IR transient that is insensitive to thermal heating and from the time-dependent frequency of vanishing ΔOD (cf. Eq. (1) and Fig. 4), we can safely extract a reliable value for the bending lifetime, i.e. $1/k_B = 220$ fs, that can be used as a constraint in the fit. The expression in Eq. (12) for the spectro-temporal evolution of the pump-induced optical density contains further the difference cross-sections $\Delta\sigma_{SB}$, $\Delta\sigma_{SL}$, and $\Delta\sigma_{hot}$. In principle, these quantities are local fitting parameters, because they will differ from one detection wavelength to another. Consequently, the fitting result will become highly ambiguous or the fitting algorithm will fail to converge, unless the frequency dependence of these cross-sections is represented in a parameterized analytic form containing a few but global fitting parameters only. As mentioned above, the thermal difference cross-section can in principle be determined independently from stationary FTIR spectra. Alternatively, it can also be obtained from the pump-induced optical density $\Delta OD(\tau, \tilde{\nu})$ at infinite pump–probe delay, for example at 8 ps. For further reference, we model the transient spectrum $\Delta OD(\infty, \tilde{\nu})$ by the following wavelength-dependent line-shape with $i = 4$:

$$g_i(\lambda) = \sum_{j=1}^{i} A_j \exp\left( -4\ln(2)\left( \frac{\lambda - \lambda_j}{\Delta\lambda_j} \right)^2 \right), \tag{15}$$

where the amplitudes, $A_j$, the center wavelengths, $\lambda_j = 1/\tilde{\nu}_j$ and spectral widths (FWHM), $\Delta\lambda_j$, are summarized in Table 1. The resulting line-shape slightly deviates from our results obtained by thermal FTIR difference spectroscopy, which could be due to some wavelength dependent spatial mismatch between the pump and the probe beams inside the sample cell. However, our stationary difference spectra differ somewhat from those reported by Iwata et al. [12] demonstrating that it is not at all an easy task to record $\Delta\sigma_{hot}$ as a function of temperature with conventional FTIR instruments and sufficient reproducibility. Therefore, we decided to normalize all pump–probe data to Eq. (15) at a delay of 8 ps, thereby facilitating an immediate reconstruction of our entire raw data set using the results compiled in Table 1 without being biased to any stationary thermal difference spectrum.

Table 1
Parameters for the cross-sections are given in the table

| Index | Parameters for $\Delta\sigma_{SB}$ | | | Parameters for $\Delta\sigma_{hot}$ | | |
|---|---|---|---|---|---|---|
| | $A_j$ | $\lambda_j$ (nm) | $\Delta\lambda_j$ (nm) | $A_j$ | $\lambda_j$ (nm) | $\Delta\lambda_j$ (nm) |
| 1 | −3.8 | 3100 | 280 | −18.607 | 2909 | 411 |
| 2 | 7.6 | 2680 | 296 | 11.64 | 2906 | 223 |
| 3 | −6.46 | 2715 | 135 | 13.105 | 2788 | 194 |
| 4 | | | | −0.649 | 2652 | 367 |

Further results obtained in the fit: $P_d = 0.01$, $f/\Phi = 61.9$, librational lifetime $1/k_L = 900$ fs and lifetime of the bending mode $1/k_B = 220$ fs.

In a next step of the fitting procedure, we also fixed the librational lifetime to the value reported in Ref. [10] and optimized in a least squares fit the quantity $\Phi$ as well as the bend–stretch and libration–stretch differential cross-sections, $\Delta\sigma_{SB}$ and $\Delta\sigma_{SL}$, whose frequency dependence was parametrized by the functional form Eq. (15). It turned out, that the variation of $\Delta\sigma_{SL}$ with the probe frequency resembled closely that of the thermal difference cross-section, i.e. $\Delta\sigma_{SL} = f\,\Delta\sigma_{hot}$. Since the temporal evolution of $\Delta OD(\tau, \tilde{\nu})$ below 1 ps delay could not reproduced to our satisfaction, the librational and bending lifetimes were now both used as a free floating parameter, while the pump-induced optical density was simplified to the expression

$$\Delta OD(\tau, \tilde{\nu}) = \Delta\sigma_{SB}(\tilde{\nu})[B] + \{f[L] + [M]\}\Delta\sigma_{hot}(\tilde{\nu}). \tag{16}$$

This still leaves a total of four global fitting parameters, namely $P_d$, $k_B$, $k_L$ and the ratio $f/\Phi$, but reduces the number of adjustable line shape parameters by a factor of 2. With these degrees of freedom in the simulation, a total of 8000 experimental data points from 200 transient differential transmission spectra evenly distributed between 0 and 8 ps had to be reproduced. The results of this final step are summarized in Table 1. Simulations of representative time-resolved pump–probe transients and frequency-resolved differential transmission spectra are shown in 2 and 3 as solid curves. The agreement between experiment and fit is excellent, in particular, when considering the very small ratio between the number of fitting parameters and the number of data points to be reproduced. Within the assumptions implicit in the model, the librational lifetime is found to be 900 fs, which is in quantitative agreement with the time constant reported by Elsaesser and coworkers

[10] for energy delocalization over many molecules following an initial bending or librational excitation. This time-window was connected by the authors to the breaking of hydrogen bonds and a macroscopic heating of the liquid. Notice that our model mimics and simplifies these dynamics by a single-step librational decay. Releasing the constraint on the bending mode lifetime did not improve the fit significantly. In fact, the value for $1/k_B = 220$ fs is also recovered when the thermalization time is fixed to ~900 fs. In particular, the early time behavior in the spectral region where the transient absorption dominates $\Delta OD(\tau, \tilde{\nu})$ below 500 fs could not be reproduced satisfactorily when a bending mode decay rate-constant larger than 1/(200 fs) was used.

### 3.3. Anharmonic bend–stretch coupling

The major result from the above simulations is the differential anharmonic bend–stretch coupling cross-section, $\Delta\sigma_{SB}(\tilde{\nu})$, which can be retrieved with the quantities $f/\Phi$ and $P_d$. This cross-section is shown in Fig. 6 as the solid curve and is compared to the linear absorption of water corresponding to the fundamental OH-stretching absorption cross-section, $\sigma_{00-10}(\tilde{\nu})$. To the best of our knowledge, the derivation of an absorption cross-section from a combination tone transition from femtosecond time-resolved mid-IR pump–probe measurements on hydrogen-bonded water is without precedent. We note that beautiful equivalent experiments were recently carried out by Graener and coworkers on free water dissolved in non-hydrogen-bonded environments such as liquid $CDCl_3$ and $C_2H_4Cl_2$ [13]. Previous complementary studies on the vibrational relaxation dynamics of liquid water have used the differential cross-sections such as those appearing in Eq. (12) as simple local fitting parameters, i.e. they were used as additional unconstrained amplitudes for the time-dependent populations for each individual detection wavelength.

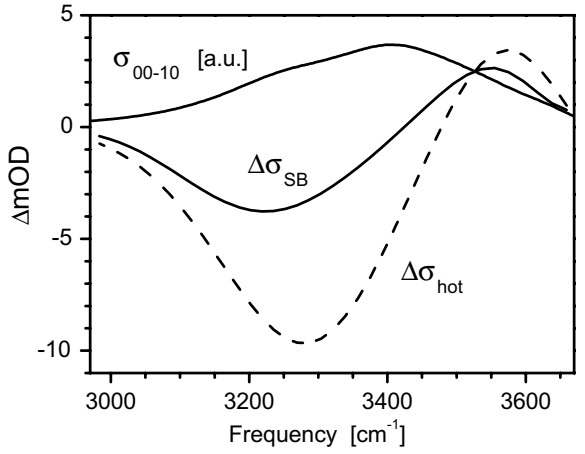


Fig. 6. Differential cross-sections for the bend–stretch anharmonic coupling, $\Delta\sigma_{SB}$, and for the low-frequency modes, $\Delta\sigma_{hot}$. For comparison, the absorption cross-section from the ground state to the first excited state of the stretching mode, $\sigma_{00-10}$, is given in arbitrary units.

Our approach to implement a parameterized analytic form for the probe wavelength dependence not only greatly reduces the total number of fitting parameters, but it also facilitates a rapidly converging global data analysis that takes into account the entire spectro-temporal response in the mid-IR at once. Such a comprehensive data treatment lends credence to the qualitative and quantitative frequency dependence of $\Delta\sigma_{SB}(\tilde{\nu})$ without having a detailed physical rationale for the actual line-shape function used to analytically represent this frequency dependence. We stress, that a data analysis which uses differential cross-sections as local fitting parameters, may result in arbitrary frequency variations including sudden sign-changes of the $\Delta\sigma_{SB}(\tilde{\nu})$ output. This makes it practically impossible to differentiate and interpret any underlying smooth (and therefore, physically significant) frequency-dependence from the fitting noise.

The most striking feature that can be identified in Fig. 6 is a shift of the OH-stretching resonance by the presence of the bending quantum to higher frequencies as compared to the pure fundamental transition. At a first glance, such a blue-shift is rather surprising considering the usual red-shifts associated with diagonal anharmonicities. However, we can estimate the off-diagonal bend–stretch anharmonicity directly from linear absorption spectra in the near infrared region below 2 μm wavelengths.

The bend–stretch combination resonance of liquid water gives rise to a rather diffuse band, which peaks near 5185 $cm^{-1}$ and has a spectral width of ~200 $cm^{-1}$. Subtracting the resonance frequency of the fundamental bending transition of the liquid of 1645 $cm^{-1}$ provides a first crude estimate for the Bohr frequency of the OH-resonance carrying a spectating bending quantum of 3540 $cm^{-1}$. The maximum of the OH-stretching band is located at 3408 $cm^{-1}$ for liquid water at room temperature. Therefore, a blue-shift of 132 $cm^{-1}$ associated with the bend–stretch off-diagonal anharmonicity can indeed be expected for pure liquid water.

Our results are however in stark contrast with recent experiments by Seifert et al. [13] on water dissolved in non-polar liquids. For such non-hydrogen bonded water molecules, an initial pump-pulse induced bending excitation leads to two pronounced bleaching signals in the OH-stretching region corresponding to the symmetric and antisymmetric OH-stretching resonances. Each component was accompanied by a transient absorption due to the bending population, which appeared clearly red-shifted to the bleach by roughly 21 $cm^{-1}$. Furthermore, such a red-shift in non-polar environments is fully in-line with the negative off-diagonal anharmonicities between the bending mode and the hydroxyl stretches derived for $H_2O$ in the gas phase [14]. Therefore, it seems plausible that the blue-shift identified from our data set on neat liquid water is intimately connected to the hydrogen-bond network.

Previous studies on the structure and the dynamics of liquid water interpreted the OH-stretching band as a dynamically averaged length and angular distribution of

$H_2O\cdots HOH$ bridges. This is because in general, the frequency of OH-vibrators engaged in $O\cdots H–O$ hydrogen bonds decreases with increasing $O\cdots O$ distance. Such a notion was further corroborated by detailed molecular dynamics (MD) simulations [15,16]. In addition, IR cavity ring down laser absorption spectroscopy by Saykally and coworkers on different size water clusters in the gas phase has demonstrated that the hydroxyl stretch resonance shifts to lower frequencies with increasing cluster size [17]. In a recent publication [18], we have taken the dielectric constant of water as an empirical measure for the hydrogen bond connectivity in the liquid network and have shown that the hydroxyl stretch resonance frequency correlates very well with the average number of hydrogen bonds per molecule. Regardless of the notion, it is quite likely that the initial pump-induced excitation of the bend induces significant changes of the average hydrogen bond angles and lengths which in turn, translate into measurable frequency shifts of the OH-stretch.

Referring to Fig. 6, the frequency shift of 260 $cm^{-1}$ between transient absorption and bleach gives an upper limit for the bend–stretch off-diagonal anharmonicity. Such a value would then require an on-average elongation of the hydrogen bridge by about 0.04 nm, as judged from the MD results by Skinner and coworkers [16]. Note however, that the OH-frequency spread for a given hydrogen bond length is already more than 150 $cm^{-1}$, i.e. comparable to the upper limit for the bend–stretch anharmonic coupling. Similarly, an angular distortion of the molecules by $\sim 10°$ would result in an equivalent blue-shift and the OH-frequency variance for a given bend-angle can easily exceed the anharmonic coupling.

By preparing the first excited state of the bending mode, the diagonal anharmonicity along the bending coordinate results in a slightly increased expectation value for the HOH angles. As a consequence, for a frozen intermolecular distance between hydrogen bonded pairs, the average angular deformation of an initially excited $H_2O$ molecule translates into a slight extension as well as a significant bending of the interconnecting $O–H\cdots O$ bridge. The combined effects must then give rise to a blue shifted hydroxyl stretching frequency of the bending excited water.

In an alternative notion, one can envision that the initial excitation of the bending mode induces the breakage of hydrogen-bridges to nearest neighbors thereby leading to a blue-shifted OH-stretching resonance typical for smaller $H_2O$ clusters with fewer hydrogen bonds. Support for such a light-induced hydrogen bond fission was observed by Fayer and coworkers for an initial OD-stretch excitation of HOD dissolved in $H_2O$ [19]. Interestingly, the spectrum of the HOD photoproduct (i.e. the spectrum associated with broken hydrogen-bonds) was characterized by an induced absorption that is also blue shifted with respect to the bleach. On a time scale of a few picoseconds, this spectrum then gradually evolved into a thermal difference absorption spectrum of HOD thereby reflecting the thermal equilibration within the hydrogen bonded network. Both observations are in full agreement with the findings presented here for neat liquid water.

## 4. Conclusions

We have presented a study on the anharmonic coupling between the bending and stretching modes in liquid water. Two-color pump–probe measurements were performed to observe the changes in the stretching mode spectral region upon excitation of the bending mode. The approach of pumping the lower energy mode and monitoring induced transmission changes of higher frequency vibrations has the advantage that populations of upper vibrational levels of the probe-transition do not change with time. Therefore, pump-induced optical densities in the spectral region of the probed mode are highly sensitive to its pumped vibration as well as to those that are transiently populated during relaxation.

The bend–stretch coupling gives rise to a transient absorption decaying directly with the bend lifetime. A comprehensive data analysis shows that the ensuing relaxation of the excess vibrational energy to LFM occurs via the librational manifold. Excitations of librations and LFM have practically the same spectral signature and can be distinguished only by their different temporal behavior. In contrast, the differential cross-section due to bend–stretch coupling is markedly different. It was shown to be blue-shifted with respect to the fundamental stretching transition, which may originate from the diagonal anharmonicity along the bending coordinate that is transferred into the bend–stretch cross-section via the hydrogen-bonded network. Alternatively, the blue-shift may originate from breakage of hydrogen-bonds caused by the initial deposition of sufficient excess energy by the pump-pulse. The perturbed hydrogen-bonded network with an on-average smaller number of H-bonds relaxes on a time scale of 900 fs, thereby establishing the hydrogen-bond connectivity typical for water at a slightly elevated temperature.

## Acknowledgement

We gratefully acknowledge financial support by the Deutsche Forschungsgemeinschaft (Grant No. Vo 593/5-1), and the ''Nederlandse Organisatie voor Wetenschappelijk Onderzoek (NOW)'' through the''Stichting voor Fundamenteel Onderzoek der Materie'' (FOM) research program.

## References

[1] T.H. Elsaesser, H.J. Bakker (Eds.), Ultrafast Hydrogen Bonding Dynamics and Proton Transfer Processes in the Condensed Phase, Kluwer Academic Publisher, Amsterdam, 2003.
[2] E.T.J. Nibbering, T. Elsaesser, Chem. Rev. 104 (2004) 1887.
[3] X.W. Hou, M. Xie, Z.Q. Ma, Phys. Rev. A 55 (1997) 3401.
[4] A.J. Lock, S. Woutersen, H.J. Bakker, J. Phys. Chem. A 105 (2001) 1238.

[5] A.J. Lock, H.J. Bakker, J. Chem. Phys. 117 (2002) 1708.
[6] O.F.A. Larsen, S. Woutersen, J. Chem. Phys. 121 (2004) 12143.
[7] N. Huse, S. Ashihara, E.T.J. Nibbering, T. Elsaesser, Chem. Phys. Lett. 404 (2005) 389.
[8] M.L. Cowman, B.D. Bruner, N. Huse, J.R. Dwyer, B. Chugh, E.T.J. Nibbering, T. Elsaesser, R.J.D. Miller, Nature 434 (2005) 199.
[9] J. Lindner, P. Vöhringer, M.S. Pshenichnikov, D. Cringus, D.A. Wiersma, M. Mostovoy, Chem. Phys. Lett. 421 (2006) 329.
[10] S. Ashihara, N. Huse, A. Espagne, E.T.J. Nibbering, T. Elsaesser, Chem. Phys. Lett. 424 (2006) 66.
[11] S. Ashihara, N. Huse, A. Espagne, E.T.J. Nibbering, T. Elsaesser, J. Phys. Chem. A 111 (2007) 743.
[12] T. Iwata, J. Koshoubu, C. Jin, Y. Okubo, Appl. Spectrosc. 51 (1997) 1269.
[13] G. Seifert, T. Patzlaff, H. Graener, J. Chem. Phys. 125 (2006) 154506.
[14] R. Lemus, J. Mol. Spectrosc. 225 (2004) 73.
[15] C.J. Fecko, J.D. Eaves, J.J. Loparo, A. Tokmakoff, P.L. Geissler, Science 301 (2003) 1698.
[16] C.P. Lawrence, J.L. Skinner, Chem. Phys. Lett. 369 (2003) 472.
[17] J.B. Paul, C.P. Collier, R.J. Saykally, J.J. Scherer, A. O'Keefe, J. Phys. Chem. A 101 (1997) 5211.
[18] D. Schwarzer, J. Lindner, P. Vöhringer, J. Phys. Chem. A 110 (2006) 2858.
[19] T. Steinel, J.B. Asbury, J. Zheng, M.F. Fayer, J. Phys. Chem. A 108 (2004) 10957.